This article was downloaded by:
On: *25 January 2011*
Access details: *Access Details: Free Access*
Publisher *Taylor & Francis*
Informa Ltd Registered in England and Wales Registered Number: 1072954 Registered office: Mortimer House, 37-41 Mortimer Street, London W1T 3JH, UK

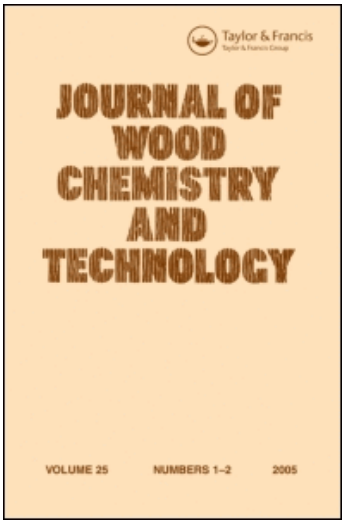

Journal of Wood Chemistry and Technology
Publication details, including instructions for authors and subscription information:
http://www.informaworld.com/smpp/title~content=t713597282

Scale of Homogeneous Mixing in Miscible Blends of Organosolv Lignin Esters with Poly(ε-caprolactone)

Yoshikuni Teramoto[a]; Seung-Hwan Lee[b]; Takashi Endo[b]; Yoshiyuki Nishio[a]
[a] Division of Forest and Biomaterials Science, Graduate School of Agriculture, Kyoto University, Kyoto, Japan [b] National Institute of Advanced Industrial Science and Technology (AIST), Biomass Technology Research Center (BTRC), Kure, Japan

Online publication date: 20 November 2010

To cite this Article Teramoto, Yoshikuni , Lee, Seung-Hwan , Endo, Takashi and Nishio, Yoshiyuki(2010) 'Scale of Homogeneous Mixing in Miscible Blends of Organosolv Lignin Esters with Poly(ε-caprolactone)', Journal of Wood Chemistry and Technology, 30: 4, 330 — 347
To link to this Article: DOI: 10.1080/02773811003714194
URL: http://dx.doi.org/10.1080/02773811003714194

PLEASE SCROLL DOWN FOR ARTICLE

Full terms and conditions of use: http://www.informaworld.com/terms-and-conditions-of-access.pdf

This article may be used for research, teaching and private study purposes. Any substantial or systematic reproduction, re-distribution, re-selling, loan or sub-licensing, systematic supply or distribution in any form to anyone is expressly forbidden.

The publisher does not give any warranty express or implied or make any representation that the contents will be complete or accurate or up to date. The accuracy of any instructions, formulae and drug doses should be independently verified with primary sources. The publisher shall not be liable for any loss, actions, claims, proceedings, demand or costs or damages whatsoever or howsoever caused arising directly or indirectly in connection with or arising out of the use of this material.

Journal of Wood Chemistry and Technology, 30: 330–347, 2010
Copyright © Taylor & Francis Group, LLC
ISSN 0277-3813 print / 1532-2319 online
DOI: 10.1080/02773811003714194

Taylor & Francis
Taylor & Francis Group

Scale of Homogeneous Mixing in Miscible Blends of Organosolv Lignin Esters with Poly(ε-caprolactone)

Yoshikuni Teramoto,[1] Seung-Hwan Lee,[2] Takashi Endo,[2] and Yoshiyuki Nishio[1]

[1]Division of Forest and Biomaterials Science, Graduate School of Agriculture, Kyoto University, Kyoto, Japan

[2]National Institute of Advanced Industrial Science and Technology (AIST), Biomass Technology Research Center (BTRC), Kure, Japan

Downloaded At: 11:56 25 January 2011

Abstract: Organosolv lignin (OSL) esters (side-chain carbon number, $n = 3$, 4, and 5) have been demonstrated to be miscible with poly(ε-caprolactone) (PCL) on a scale (20–30 nm) for detecting glass transition temperature (T_g) by differential scanning calorimetry (*Polym. J.* 2009, 41(3), 219–227). Further precise quantification of homogeneity was conducted for the OSL propionate (OSL-Pr, $n = 3$)/PCL and OSL butyrate (OSL-Bu, $n = 4$)/PCL blends by means of dynamic mechanical analysis (DMA) and solid-state nuclear magnetic resonance (NMR). DMA revealed a composition-dependent T_g for these blend samples, which implies the attainment of an intimate mixing of the ingredients on a scale of ≤15 nm. From the measurements of proton spin-lattice relaxation times ($T_{1\rho}{}^H$) using solid-state NMR, the blends were estimated to be substantially homogeneous on a scale of ∼6 nm. But the equalization of the $T_{1\rho}{}^H$ for the components of OSL-Pr/PCL was not remarkable; that is, the constituents of OSL-Pr/PCL were relatively imperfectly miscible with each other.

Keywords: Dynamic mechanical analysis, homogeneity, miscibility, organosolv lignin ester/poly(ε-caprolactone) blends, solid-state NMR

INTRODUCTION

Currently, studies on bioethanol production from lignocellulosics are being actively pursued.[1–4] Even though the lignin by-product is considered merely as a heat resource for the process in the present circumstances, its effective

Address correspondence to Yoshikuni Teramoto, Division of Forest and Biomaterials Science, Graduate School of Agriculture, Kyoto University, Kitashirakawa Oiwak-cho Sakyo-ku, Kyoto 606-8502, Japan. E-mail: teramoto@kais.kyoto-u.ac.jp

application as high value-added products will contribute to cost reduction of total system for biofuel production. Generally, however, the utilization of lignin as a solid material is constrained by poor film formability and less thermal moldability due to its molecular architecture and intermolecular interactions in itself. Blending of lignin with other polymers is a possible way to modify the thermal and other physical properties of the target lignin and to obtain new polymeric materials having wide-ranging properties.[5–11]

Physical properties of polymer blends are influenced ultimately by the level of mixing. In this perspective, various techniques have been employed to investigate the level of mixing of polymer blends,[12–20] including microscopy, thermal analysis, dynamic mechanical analysis (DMA), and spectroscopic measurements. Differential scanning calorimetry (DSC) is one of the most widely used techniques for evaluating miscibility, on a scale of 20–30 nm, in terms of the cooperative motion of polymer segments at temperatures close to the glass transition temperature (T_g).[12,15,17] DMA can quantify a somewhat fine scale of homogeneity and reveal a single T_g in polymeric mixtures with domain sizes smaller than ca. 15 nm.[12,15,17] Solid-state nuclear magnetic resonance (NMR) spectroscopy is a powerful technique that has been utilized to analyze the miscibility, phase structure, and heterogeneity of polymer mixtures on a molecular scale.[16,18–20] A useful proton spin-relaxation time that can be obtained in solid-state ^{13}C NMR techniques is the spin-lattice relaxation time in the rotating frame ($T_{1\rho}{}^{H}$). The length scale of heterogeneity, usually on a scale of a few nanometers, can be approximated from the value of $T_{1\rho}{}^{H}$ to allow assessments of compositional heterogeneity on length scales limited by spin diffusion.[16,18–20]

In our previous study,[11] basic miscibility estimation was conducted for essentially biodegradable blends of esterified organosolv lignin (OSL) (the carbon number of the introduced acy unit, $n = 2$, 3, 4, and 5) with poly(ε-caprolactone) (PCL) through morphological observation, DSC, and infra-red spectroscopy. On a scale of a few micrometers, atomic force microscopy indicated that no remarkable phase separation occurred in the blends of OSL propionate (OSL-Pr, $n = 3$), OSL butyrate (OSL-Bu, $n = 4$), and OSL valerate (OSL-Va, $n = 5$). DSC revealed a composition-dependent shift in T_g for any blend of the OSL esters ($n = 3$, 4, and 5) with PCL; thus these three systems can be regarded as miscible on the T_g-detection scale (20–30 nm).[12,15,17]

For the miscibility attainment, a structural similarity appears to be an important factor[11,21,22]; namely OSL-Bu and OSL-Va have, most abundantly, the same structural unit as that of PCL (C−C−O−(CO)−C−C−C or C−O−(CO)−C−C−C−C), if the aliphatic carbon atoms neighboring aliphatic hydroxyl groups are taken into account. In OSL-Pr, which contains the structure O−(CO)−C−C, however, there is less frequency of occurrence of the same structural unit as that of PCL even when the aliphatic hydroxyl groups are esterified. In fact, for the OSL-Pr/PCL blend, an abrupt T_g-elevation with increasing the OSL ester component was observed,[11] which reflects that more

Downloaded At: 11:56 25 January 2011

content of the lignin ester was required for the shift in T_g. Furthermore, in observations of isothermal crystallization behavior of the PCL component for the OSL-Pr/PCL blend,[11] a spherulite texture was generally small and distorted, and worse in contrast; such a non-uniform morphology might be ascribed to a relatively lower degree of miscibility of this OSL ester with PCL.

Such a subtle difference in the mixing heterogeneity between polymer blends will affect not only the physical property as bulk materials but also the stability of practical thermal-processing such as injection and inflation moldings because the microscopic heterogeneity might play a role of defect sites. In the present study, we devoted refining efforts to further precise quantification of the scale of homogeneity in the OSL-Pr ($n = 3$)/PCL and OSL-Bu (n = 4)/PCL blends by means of DMA and solid-state NMR.

EXPERIMENTAL

Materials

Downloaded At: 11:56 25 January 2011

Organosolv lignin (OSL) was purchased from Aldrich Chemical Co. The numbers of functional groups and molecular weights were determined by ^{1}H NMR spectroscopy and gel permeation chromatography (GPC), respectively, in a procedure similar to that reported previously.[11] The numbers of functional groups (per phenyl propane unit, PPU) of OSL are as follows: total OH, 1.23; aliphatic OH, 0.61; aromatic OH, 0.62; methoxyl (OMe), 1.06. The weight-average molecular weight (M_w) and molecular weight distribution (M_w/M_n, M_n is the number-average molecular weight) of OSL were 3.36×10^3 and 3.52, respectively. Poly(ε-caprolactone) (PCL) was purchased from Wako Pure Chemical Industries, Ltd.; its nominal molecular weight was 40,000. Other solvents and chemicals used in this study were purchased from Wako Pure Chemical Industries, Ltd.; these were all of guaranteed reagent grade and used without further purification.

Sample Preparation

OSL was esterified with an acid anhydride appropriate for the objective product in pyridine containing 4-dimethylaminopyridine, in a manner similar to that used in the previous study.[11] The respective OSL esters were fully substituted ones. The M_w of the respective OSL esters was determined by GPC: 3.43×10^3 (OSL-Pr) and 4.30×10^3 (OSL-Bu). The molecular weight distributions for the two products were 3.20 (OSL-Pr) and 3.19 (OSL-Bu).

OSL ester/PCL polymer blends were prepared in film form from mixed polymer solutions by solvent evaporation. Chloroform was selected as a common solvent. 1-wt% solutions of OSL ester and PCL were prepared separately and mixed with each other in the desired proportions. After stirring over a

time period of 24 h at 25°C, each mixed solution (transparent but brown) was poured into a Teflon tray and a film sheet was prepared by solvent evaporation at 25°C and atmospheric pressure. The as-cast film samples were dried at 40°C in vacuo for 12 h. Cast films of plain PCL were also obtained in a similar manner. Film specimens ca. 0.1 mm thick were prepared by hot-press molding (150°C, 5 MPa) of the cast samples. The specimens were stored at 20°C in a desiccator for ∼2 months.

Measurements

DSC was performed by using a PerkinElmer DSC7. The measurements were carried out on 7-mg film samples under a helium atmosphere after calibrating the temperature readings with an indium standard. The samples were heated from –150°C to 120°C at a scanning rate of 20°C/min. The melting temperature (T_m) and the enthalpy of fusion (ΔH_f) were determined from the maximum and the area of the melting endotherm, respectively, in the first heating scan.

DMA measurements were conducted by using a Seiko DMS6100/EXSTAR6000 apparatus for the film specimens. Strips of rectangular shape (20×4 mm^2) cut from the film specimens were used for measurements of the temperature dependence of the dynamic storage modulus (E') and loss modulus (E''). The measuring conditions were as follows: temperature range, −150–280°C; scanning rate, 2°C/min; oscillatory frequency, 10 Hz.

Wide-angle X-ray diffraction (WAXD) measurements were also made for the film specimens with a Rigaku Ultima-IV diffractometer at 20°C in a reflection mode. Nickel-filtered CuKα radiation was used at 40 kV and 40 mA. The diffraction intensity profiles were collected in the range of $2\theta = 10$–30°.

Solid-state NMR experiments were carried out at 20°C with a Varian Unity INOVA 400 WB NMR apparatus operated at a ^{13}C frequency of 100 MHz, using powdery OSL ester samples stored at 20°C for ∼2 months after synthesis and the aforementioned film specimens of PCL and blend samples. The magic angle spinning rate was approximately 5 kHz. ^{13}C CP/MAS spectra were measured with a contact time of 1 ms. A 90° pulse width of 4.0 μs was used with 2048 FID signal accumulations. In the measurements of proton spin-lattice relaxation times in the rotating frame ($T_{1\rho}{}^{H}$), a contact time of 0.1 ms was used and a proton spin-locking time τ ranged from 1 to 40 ms.

RESULTS AND DISCUSSION

Thermal History of Film Specimens Used in the Present Study

For film specimens of the present two OSL ester/PCL blend series, attention should be given to the thermal history and also to the crystallizability of the

Downloaded At: 11:56 25 January 2011

PCL component. Generally, in blends of an amorphous/crystallizable polymer pair, A/C, if the thermal processing is conducted above the glass transition of A, that is, $T_{proc} > T_g(A)$, and above the melting point of C, $T_{proc} > T_m(C)$, both the phase equilibrium at T_{proc} and the crystallization of C upon cooling must be considered. The potential miscibility is usually attained in the molten state. At $T < T_m(C)$ the crystallizable constituent C may supercool or crystallize ($T > T_g(blend)$). The amorphous A component is normally expelled from the growing crystal of C. Such a crystallization of one component can not be a factor to rebut the miscibility attainment of the polymer blends concerned. However, in the case of a miscible system, the crystallization varies the fraction of an amorphous phase comprising the mixed two polymers in the solid material, according to both the kinetic and thermodynamic conditions of the solidification.

In the preceding paper,[11] to determine T_g of the OSL ester/PCL blends we conducted DSC analysis in the second heating scan after rapid cooling (500 K/min) from a molten state. It should be noted that DSC thermograms of some compositions rich in the OSL ester component represented no endotherm ascribable to a fusion of PCL crystal, without indicating even a crystallization possible in the heating scan. Other intermediate compositions exhibited a fusion signal coming principally from the cold-crystallization of PCL that occurred after onset of the glass transition of these samples on heating.[11] These observations of generally slower crystallization for the PCL component reflect a good miscibility of the blend samples. On the other hand, the film specimens used in this study preserve other thermal history (stored at 20°C for ~2 months after thermal molding) than that for the previous T_g determination. All DSC thermograms in the first heating scan for the specimens show a melting endotherm centered at ~60°C and no cold-crystallization exotherm, indicating sufficient development of PCL crystal in the storage period. Eventually, the film specimens used here contain less amount of amorphous PCL due to the crystallization of this component, in comparison with the samples provided for the T_g measurement by means of DSC in the second heating.

Using DSC thermograms in the first heating scan, the crystallinity index X_c for the present specimens can be calculated per net weight of PCL or blend material, from the following equations

$$X_c(\text{PCL}) = \Delta H_f/(\Delta H_f^0) \tag{1}$$

$$X_c(\text{blend}) = \Delta H_f/(\Delta H_f^0 \times f) \tag{2}$$

where $\Delta H_f^0 = 136$ J/g[23] is the heat of fusion of 100% crystalline PCL and f is the weight fraction of the PCL component. The result is listed in Table 1. As shown there, the index X_c(PCL) became larger and T_m lowered with an increase in the OSL ester content in the blend. The precise reason for the increase in X_c(PCL) is unknown at present, but it may be possible that the OSL ester

Downloaded At: 11:56 25 January 2011

Table 1. Characterization of developed PCL crystal for the film specimens used in this study by means of DSC (first heating scan) and WAXD

Sample	T_m/°C	X_c(PCL)	X_c(blend)	FWHM ($2\theta = 21.3°$)/°
OSL-Pr/PCL = 25/75	62.6	0.765	0.574	0.389
OSL-Pr/PCL = 50/50	60.3	0.773	0.367	0.493
OSL-Pr/PCL = 75/25	59.0	0.855	0.214	0.534
OSL-Bu/PCL = 25/75	62.9	0.750	0.562	0.357
OSL-Bu/PCL = 50/50	60.4	0.773	0.386	0.463
OSL-Bu/PCL = 75/25	58.1	0.808	0.202	0.519
PCL	64.0	0.696	0.696	0.453

molecules, more or less having a structurally similar alkyl ester to PCL, act as a rather nucleating agent for the partial crystallization of the PCL component. On the other hand, the lowering of T_m seems to be related to a reduction in lamella size of the developed PCL crystal with increasing OSL ester content. Table 1 also tabulates the full-width at half maximum (FWHM) of a WAXD peak at $2\theta = 21.3°$ derived from the (110) crystallographic plane of PCL crystal. As seen in this table, FWHM increases with increasing OSL ester content. This increase indicates an overall reduction in size and/or regularity of the formed PCL crystal with increasing OSL ester content.[24] Such a morphological effect might cause the lower T_m. Meanwhile, the index X_c(blend) naturally decreased with decreasing PCL content.

Downloaded At: 11:56 25 January 2011

Transition Behavior of OSL Ester/PCL Blends Evaluated by DMA

Through the use of DMA, an assessment of the extent of mixing between blend components is facilitated because of the higher sensitivity of the method compared to DSC. Via DMA, three parameters are obtained as a function of temperature: the storage modulus (E'), the loss modulus (E''), and the loss tangent tan δ. In the T_g region, a maximum appears in each of the E'' and tan δ versus temperature, while there is a decrease in the E' due to loss in stiffness, so that the plot of E' versus temperature reveals a drop. Consequently, the three parameters that can be measured by DMA can be used to determine T_g. These parameters are sensitive to many processes,[25] including structural heterogeneities and molecular motions, so that changes in the immediate environment of a given polymer chain caused by intimate mixing can be recognized from changes in location of the E'' and tan δ maxima and the midpoint of the E' drop.

Figure 1 shows the temperature dependence of the dynamic storage modulus E' and loss modulues E'' for the two blend series, OSL-Pr/PCL and

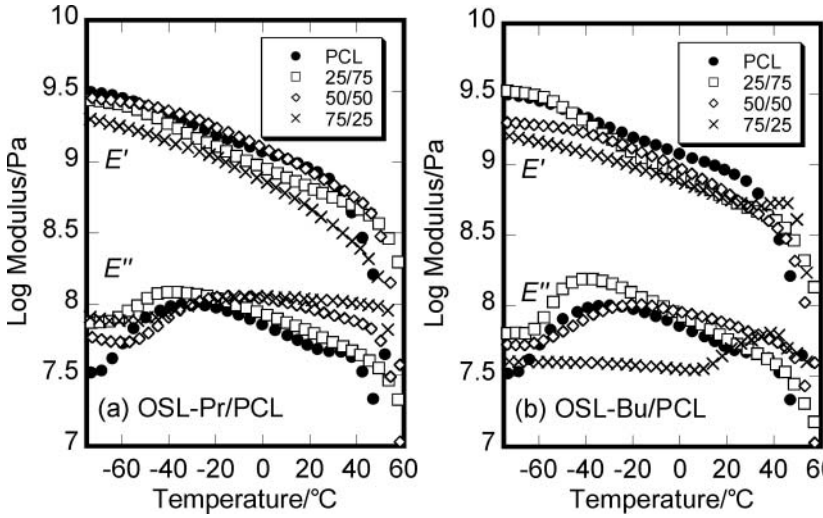

Figure 1. Temperature dependence of the dynamic storage modulus E' and loss modulus E'' for (a) OSL-Pr/PCL and (b) OSL-Bu/PCL blends. The corresponding data for a PCL homopolymer film is also included for comparison.

Downloaded At: 11:56 25 January 2011

OSL-Bu/PCL, containing 25, 50, and 75 wt% OSL ester. For comparison, the figures also include the corresponding data for a PCL homopolymer film, but do no data for OSL esters *per se*, due to the lack of sufficient moldability into a film sheet. As is evident here, the plain PCL film exhibits a dispersion peak centered at $\sim -30^{\circ}$C in the E'' versus temperature curve. This dispersion signal may be associated with the glass transition of the homopolymer. However, the E'' peak is located at a higher temperature compared with the T_g (-65°C) determined by DSC in the second heating scan,[11] indicating that the two analytical tests respond somewhat differently to the same relaxation process.[26] Also, there is another possible explanation ascribable to a higher PCL crystallite content for the specimen used here: the X_c(PCL) value was estimated to be 0.696 (Table 1) in the DSC first heating scan, larger than 0.572 obtained in the second heating. Thus the T_g-increase stated above might be caused by shortening of amorphous zones between crystallites and resulting stresses onto the amorphous chain sequences, in consequence of the enhanced crystallization process.[25] Following the termination of the glass transition on heating, the micro-Brownian motions of PCL appear to become more and more conspicuous with increasing temperature, and, above 50°C the values of E' and E'' were out of the measurement range. This is due to occurrence of the melting of PCL crystal.

On introducing 25 wt% OSL esters into the PCL, the E''-peak maximum was slightly moved to a lower temperature, but the onset of the transition on heating appeared at a higher temperature than in the situation of the plain PCL.

The lowering shift of the E''-peak maximum may be attributed to the relatively regular PCL crystallites of the OSL ester/PCL = 25/75 blends (see smaller FWHM in Table 1); the regularly sized crystallites could impose rather lesser restraint on the amorphous phase.[25] Further incorporation of OSL esters gave rise to a definite shift of the E'' peak toward the higher temperature side, as exemplified in Figure 1, although the transition signal was often broadened. T_g values of the blends were estimated from temperature reading for the maximum location of the respective E'' peaks and plotted against the OSL ester content in Figure 2. In the figure, variations of the T_g determined by DSC (second heating scan)[11] were also illustrated for the two miscible blends of the OSL esters. An elevating tendency common to both sets of the new T_g data (by DMA) with the addition of the OSL ester component is roughly consistent with the DSC result, but the values were rather higher than those determined by DSC. This discrepancy in T_g evaluation can be attributed largely to the difference in thermal history between the sample specimens used for DMA and those for DSC: the specimens provided for DMA contained a smaller amount of PCL amorphous chains due to the crystalline development, as is described already. Thus the present DMA study supports again that the two blend systems are essentially miscible from the viewpoint of T_g behavior and, further, ensures a mixing scale of less than ca. 15 nm[12,15,17] between the OSL ester and PCL components.

Concerning the OSL-Pr/PCL series, however, a T_g elevation at the 75/25 composition was less prominent compared with the case observed for the

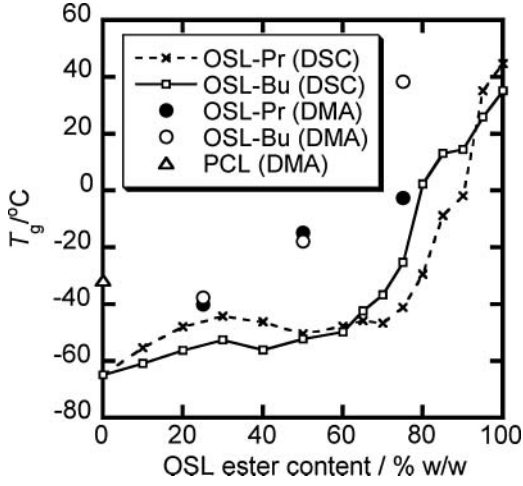

Figure 2. T_g versus composition plots for blends of OSL-Pr and OSL-Bu with PCL, determined from reading of the temperature position of an E''-peak maximum. Variations of T_g determined by DSC (second heating scan) are also illustrated for comparison by using line-drawing.

Downloaded At: 11:56 25 January 2011

OSL-Bu/PCL series. Therefore, the latter blend system may be considered to be superior in the degree of miscibility to the former one. In this connection, as shown in Figure 2, the DSC data of T_g for the OSL-Bu/PCL system provided a more continuous ascent with increasing OSL ester content ($\geq$60 wt%), differing from an abrupt rise of T_g observed for the OSL-Pr/PCL blends rich in OSL-Pr ($\geq$75 wt%). As has been pointed out in the preceding paper,[11] in OSL-Pr, there is less frequency of occurrence of the same structural unit as that of PCL even if the aliphatic hydroxyl groups are esterified. This may be why more content of the OSL-Pr component was required for the clear T_g elevation of the blends.

Another specific remark on the dynamic mechanical data is as follows. In contrast to the viscoelastic behavior of PCL alone, the introduction of OSL esters into PCL basically gave rise to a slight diminution of the modulus E' in the overall temperature range of the measurement. This apparently negative synergism in stiffness observed for the miscible blend materials is attributable principally to the decrease in PCL crystallite content in them. Generally, crystallites act as crosslinks by tying segments of many chain-molecules together and have very high moduli compared to the amorphous parts.[25] Thus, such a filler effect of the PCL crystallite should be reduced with increasing OSL ester content in the blends. Another factor is the relatively lower molecular weight ($M_w = 3.43 \times 10^3$ (OSL-Pr) and 4.30×10^3 (OSL-Bu)) of the OSL ester ingredients. These molecular weights are not high enough to be of interest for applications where mechanical properties such as modulus of toughness are important.[25] Actually, it was difficult to obtain fairly tough film sheets of the neat OSL esters by thermal molding or solution casting.

Downloaded At: 11:56 25 January 2011

Homogeneity in OSL Ester/PCL Blends Estimated by NMR Spectroscopy

Solid-state NMR spectroscopy is a useful tool for characterization of multicomponent polymer systems, especially powerful for estimating the scale of homogeneity in a polymer-polymer mixing state.[16,18–20] For example, some information about interactions between the constituent polymers is often obtainable at the molecular level ($\leq$1 nm) through analysis of ^{13}C CP/MAS NMR spectra. From the quantification of the proton spin-lattice relaxation time in the rotating frame, $T_{1\rho}{}^{H}$, it is possible to evaluate an upper limit in heterogeneity usually on a scale of a few nanometers. In this present study, these NMR techniques were employed for further characterization of the OSL ester/PCL blends, which were judged by DMA to provide an intimate mixing of the ingredients on a scale of $\leq$15 nm.

Figure 3 shows ^{13}C CP/MAS NMR spectra measured for powdery samples of OSL-Pr and OSL-Bu and the film specimens of PCL and its blends with a composition of 50/50 in the weight ratio. Relatively broad resonance for the OSL esters compared to that for PCL reflects the structural heterogeneity of these lignin derivatives and their amorphous nature. Generally, broadening of

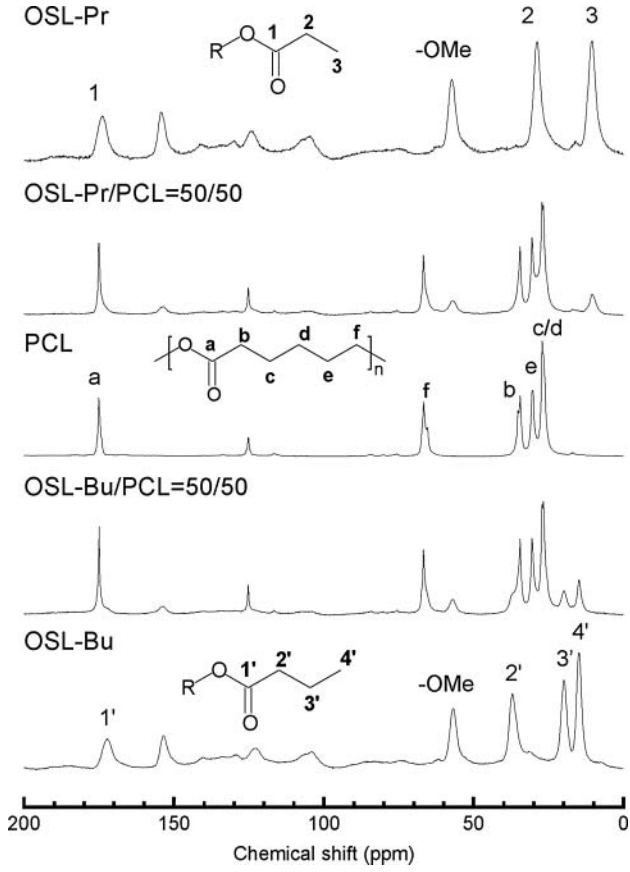

Figure 3. Solid-state ^{13}C CP/MAS NMR spectra of OSL-Pr, OSL-Bu, PCL, and their 50/50 blends.

NMR signals observed for polymers in the amorphous state is due to an inhomogeneous distribution of isotropic chemical shifts, which can be assigned to static fluctuations of bond or torsion angles. The ^{13}C resonance peaks for PCL were assigned according to literature data.[22] As regards the spectra of the OSL esters, the peak assignment was made by reference to NMR data obtained for solutions of esterified pine kraft lignins in dimethyl sulfoxide-d_6.[27] Table 2 summarizes chemical shifts of the ^{13}C resonances observed for OSL-Pr, OSL-Bu, PCL, and their 50/50 blends. In the spectra of the blend specimens, the intensities of resonance peaks derived from the lignin component were considerably smaller mainly due to the broadening effect.

In general, if two different polymers interact mutually on a molecular level (less than 1 nm) in the binary blend, the electron density around the

Downloaded At: 11:56 25 January 2011

Table 2. Assignment and ^{13}C chemical shifts (ppm) of ^{13}C CP/MAS NMR spectra for OSL-Pr, OSL-Bu, PCL, and their blends with a 50/50 composition

Carbon	OSL-Pr	OSL-Pr/ PCL = 50/50	PCL	OSL-Bu/ PCL = 5050	OSL-Bu
1	173.7	NE			
2	29.0	NE			
3	10.5	10.5			
–OMe	57.3	56.9			
a		175.0	175.0	175.0	
b		34.6	34.6	34.6	
c/d		27.3	27.2	27.2	
e		30.6	30.5	30.6	
f		66.9	66.8	66.9	
1′				NE	172.3
2′				NE	37.0
3′				19.8	20.0
4′				14.9	14.9
–OMe				56.9	56.8

NE, not evaluated because of overlapping of plural resonances.

Downloaded At: 11:56 25 January 2011

carbons bearing the interacting groups is perturbed, so that there should be some significant changes in chemical shift and/or line shape in a ^{13}C NMR spectrum of the blend, in comparison with those of their respective homopolymers.[16,19] In the present study, however, as seen in Table 2, we found no appreciable change within the limits of resolution; or rather, the ^{13}C CP/MAS NMR spectra appeared to be made up by almost simple superposition of the spectra of both homopolymers. There may be nothing surprising for no shift of the resonances assigned to the PCL component, because these resonances correspond to those of highly crystallized PCL and the blend miscibility is usually attained in the amorphous state. Nonetheless, the NMR spectra measurements provided no evidence supporting the presence of a specific intermolecular interaction between OSL ester and PCL molecules in the blends concerned.

As it is well established, an estimation of the domain size in polymer blends on a scale of a few nanometers is possible from the $T_{1\rho}^{H}$ measurements conducted in an interrupted CP/MAS NMR experiment.[16,18–20] $T_{1\rho}^{H}$ values can be obtained practically by fitting of the decaying carbon intensity to the following exponential equation:

$$M(\tau) = M(0)\exp(-\tau/T_{1\rho}^{H}) \tag{3}$$

where $M(\tau)$ is the magnietization intensity observed as a function of the spin-locking time τ. If two different polymers are in a highly miscible state in the

Table 3. $T_{1\rho}^{H}$/ms values for OSL esters, PCL, and OSL/PCL (50/50) blends, determined from the decay plots given in Figure 4

	OSL-Pr/PCL		OSL-Bu/PCL	
Weight ratio of OSL ester/PCL	OSL-Pr (OMe)	PCL (**Cf**)	OSL-Bu (OMe)	PCL (**Cf**)
100/0	25.9		24.0	
50/50	15.3	7.3[a]/49.2[b]	13.6	10.9[a]/50.5[b]
0/100		7.0[a]/50.7[b]		7.0[a]/50.7[b]

[a]Determined from a fast decay signal associated with the amorphous phase.
[b]Determined from a slow decay signal associated with the crystalline phase.

Downloaded At: 11:56 25 January 2011

binary blend, the $T_{1\rho}^{H}$ values for different protons associated with the respective components are expected to be equalized to each other by spin diffusion, as an ideal case. Figure 4 illustrates the decay behavior of ^{13}C resonance intensities for powdery OSL esters and film specimens of PCL homopolymer and the 50/50 blends. In this experiment, we monitored the resonance peak of OMe carbon in the OSL esters and that of carbon **f** in the PCL component, taking into consideration their good resolution.

For the OSL ester components, from the slope of the semilogarithmic plot of the relative intensity versus τ, a $T_{1\rho}^{H}$ value is determined successfully as the time constant of the relaxation process. As can readily be seen from the plots in Figure 4, the ^{1}H-spin diffusion of the respective OSL ester components is noticeably affected by that of the PCL component in the blends. The result of quantifications of $T_{1\rho}^{H}$ for the samples examined is summarized in Table 3.

In estimations of $T_{1\rho}^{H}$ for plain PCL and this polymer component in the blends, a trouble was the attention to the crystalline development of the polymer. As has been already shown in Table 1, the crystallinity per gram PCL in the blends was even higher than that of plain PCL. In light of the high crystallinity of the PCL component, the proton spin-lattice relaxation behavior in the rotating frame should be depicted by a bi-exponential decay function:

$$M(\tau) = M(0, \text{fast})\exp(-\tau/T_{1\rho,\text{fast}}^{H}) + M(0, \text{slow})\exp(-\tau/T_{1\rho,\text{slow}}^{H}) \qquad (4)$$

This decay function fitted the relevant experimental data well, as exemplified in Figure 4c. This figure indicates a bi-exponential obedience in the truest analysis ($R^2 = 0.999$) in comparison with the single-exponential fitting ($R^2 = 0.995$). Thus, $T_{1\rho}^{H}$ values for the specimens of PCL and its blends with OSL esters were determined through a regression analysis by Eq. (4), and the result is also included in Table 3. It is natural to assume that the shorter $T_{1\rho}^{H}$ component is

Downloaded At: 11:56 25 January 2011

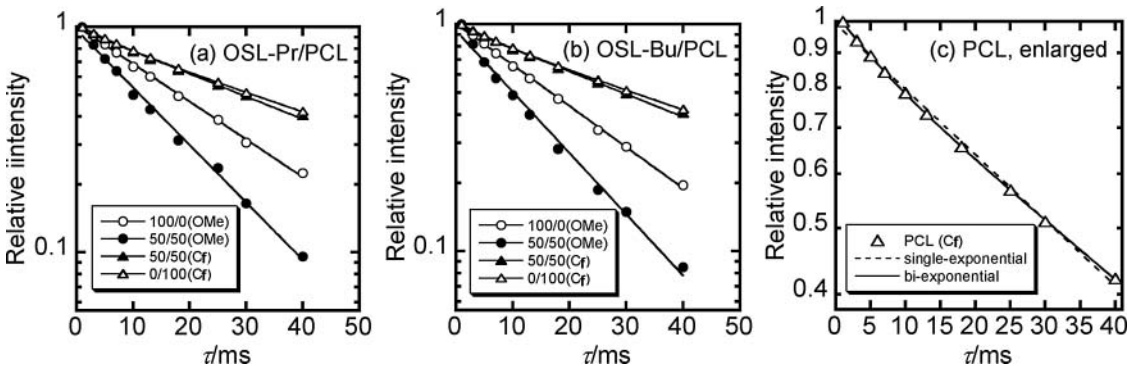

Figure 4. Semilogarithmic plots of the decay of ^{13}C resonance intensities as a function of spin-locking time τ, for OSL-Pr, OSL-Bu, PCL and their 50/50 blends. In part (c), the decay of the **Cf** signal of plain PCL is shown on an enlarged scale, to indicate a bi-exponential obedience in the truest analysis ($R^2 = 0.999$) in comparison with the single-exponential fitting ($R^2 = 0.995$).

Table 4. Fraction of the longer $T_{1\rho}^{H}$ component, $M(0, \text{slow})$, relative to the total intensity $M(0)$ to be decayed, estimated as a measure of the degree of PCL crystallinity

Sample	$M(0, \text{slow})/M(0)$
OSL-Pr/PCL = 50/50	0.898
OSL-Bu/PCL = 50/50	0.881
PCL	0.839

attributed to the amorphous phase of PCL and the longer one is associated with the rigid crystalline phase of PCL.

The intensity fraction of the slow decay component, $M(0, \text{slow})$, relative to the total intensity $M(0)$, was calculated, and the data are listed in Table 4. The fraction ($M(0, \text{slow})/M(0)$) can virtually be regarded as the PCL crystallinity, and the values obtained were larger for the blends than that for the unmixed PCL. This trend is the same as that observed for the crystallinity estimated by DSC. However, the crystallinity listed in Table 1 is based on the calorific quantity of energy required to melt the crystals, while the crystallinity determined with NMR is based on the difference in chain mobility between a rigid crystalline phase and a somewhat distended, mobile amorphous phase.

Relaxation times of $T_{1\rho}^{H} = 25.9$ and 24.0 ms were evaluated for the unblended OSL-Pr and OSL-Bu samples, respectively, and for the plain PCL, $T_{1\rho}^{H} = 7.0$ ms was obtained for the amorphous phase (see Table 3). As to the respective binary 50/50 blends, $T_{1\rho}^{H}$s of the two polymer components (amorphous) did not perfectly coincide with each other, but they got partially close to each other between the respective original values; namely $T_{1\rho}^{H}$ values of the OSL-Pr and OSL-Bu components diminished to 15.3 and 13.6 ms, respectively, and correspondingly, that of the amorphous PCL component rose to 7.3 and 10.9 ms. Here, it should be noted that $T_{1\rho}^{H}$ values expected for the above two 50/50 compositions are 15.6 (OSL-Pr/PCL) and 14.8 ms (OSL-Bu/PCL), when prorated by linear approximation considering the PCL crystallinity (from NMR), these values being fairly close to those determined for the OSL ester components. From these observations, eventually, it seems reasonable to assume that the two constituent polymers of the respective blends are mixed with each other to a considerable extent, in a range where the mutual ^{1}H-spin diffusion is permitted over a period of ~15 ms. However, the degree of $T_{1\rho}^{H}$-shift toward the equalization was more prominent in the OSL-Bu/PCL blend than that in the other employing OSL-Pr. This may support the view that the structural similarity is contributory to the attainment of more intimate mixing in the OSL ester/PCL systems.[11,17,22] In the present comparison, OSL-Pr, rather than OSL-Bu, has a lower content of the same unit as that of PCL in the molecular structure.

Downloaded At: 11:56 25 January 2011

An effective distance (L) over which spin diffusion can proceed in a time $T_{1\rho}^{H}$ is represented in the following form[28]:

$$L \approx (6DT_{1\rho}^{H})^{1/2} \tag{5}$$

where D is the spin-diffusion coefficient, which depends on the average proton to proton distance as well as on the dipolar interaction. For the spin-diffusion coefficient a value of $\sim 8 \times 10^{-16}$ m^2/s is expected to be typical in rigid organic systems.[29] However, for the diffusion coefficient in a mobile amorphous PCL material, a lower value may be assumed[30] and, for example, a value $D = 0.5 \times 10^{-16}$ m^2/s is probably a reasonable estimate.[31] In the present relaxation measurements for the blends, no component corresponding to the respective pristine OSL esters was observed, so that the upper limit for the size of the OSL ester domains can be estimated from Eq. (5), as follows. Using the coefficient $D = 8 \times 10^{-16}$ m^2/s and the $T_{1\rho}^{H}$ data (15.3 and 13.6 ms for OSL-Pr and OSL-Bu, respectively) for the 50/50 blends, we obtained the maximum average domain size of OSL-Pr and OSL-Bu as 6.1 and 5.7 nm, respectively; in this calculation, we took into consideration that in the usual CP method, the D should be scaled by a factor of 1/2 because half of the cross-polarization time accounts as an effective mixing time.[32] These values are definitely smaller than L values estimated for the neat OSL esters ($L = 7.7$ and 7.4 nm for plain OSL-Pr and OSL-Bu, respectively). This decrement of L by blending is interpreted as due to an inhibitory effect on the ^{1}H spin-diffusion, arising from the close approach of a certain amount of mobile PCL molecules to the OSL ester component. Thus $\sim$6 nm is evaluated as the upper limit for the size of the OSL ester domains in the blends.

The $T_{1\rho}^{H}$ relaxation of PCL in the blends seems more complicated. $T_{1\rho}^{H}$ data for the amorphous PCL component, 7.3 and 10.9 ms in the blends with OSL-Pr and OSL-Bu, respectively, are rather close to $T_{1\rho}^{H} = 7.0$ ms obtained for the unblended PCL sample as reference (see Table 3). Two reasons may be invoked to explain the observation of $T_{1\rho}^{H}$ behavior for PCL in the blends: one is heterogeneity in a scale of several nanometers, and the other is a motional effect even in situation of homogeneity.[33] Regarding the latter, as has been pointed out above, the PCL amorphous component is much more mobile than the OSL esters at ambient temperature. Therefore, the molecular motions of PCL would be responsible for interfering with the spatial transport of magnetization among protons, even though the spin diffusion is potentially mediated by dipolar interactions between neighboring spins belonging to the mutually different components of the blends.[34] To confirm this, we should perform the $T_{1\rho}^{H}$ measurement at temperatures much lower than T_g of the blend systems to reduce the motional effect. Such a study has not yet been done due to some difficulties of the thermo-regulated experiment. However, it seems true in the present work that OSL-Pr shows a comparatively lower degree of miscibility

Downloaded At: 11:56 25 January 2011

with PCL, as is rationalized by the larger difference between the $T_{1\rho}^{H}$ values estimated for the OSL-Pr and PCL amorphous components in the blend.

CONCLUSIONS

By means of DMA and solid-state NMR, an attempt was made to precisely quantify the scale of homogeneity in the OSL-Pr/PCL and OSL-Bu/PCL blends; these two blends have been judged to be miscible from DSC analysis in the previous study.

In the DMA measurements, these blends exhibited a systematic elevation of T_g (E''-peak position) with an increase in the OSL ester content, and the homogeneity of the blend constituents was regarded as being on a scale of less than 15 nm.

In the ^{13}C CP/MAS NMR spectra measurements, no significant shift of resonance signals accompanied the blending, which reveals no occurrence of a specific intermolecular interaction between the respective two constituent polymers. From the quantification of $T_{1\rho}^{H}$, undoubtedly, the OSL esters and PCL were seriously affected by each other in their ^{1}H-spin diffusion behavior in the amorphous phase of the respective binary blends. Therefore, it can be concluded that the size of heterogeneity in the blends is fairly small, less than ~6 nm, to permit effective spin diffusion across the different polymer constituents. However, the degree of $T_{1\rho}^{H}$-shift toward the equalization was more remarkable in the OSL-Bu/PCL blend than that in the other employing OSL-Pr; this may support the view that the structural similarity is contributive to the attainment of more intimate mixing in the OSL ester/PCL systems.

The present study revealed that nanoscopically homogeneous composite materials based on lignin can be designed via a simple lignin esterification. Such hybridization is an approach of great promise to considerable improvement for poor film formability of lignin and its derivatives.

Downloaded At: 11:56 25 January 2011

REFERENCES

1. Farrell, A.E.; Plevin, R.J.; Turner, B.T.; Jones, A.D.; O'Hare, M.; Kammen, D.M. Ethanol can contribute to energy and environmental goals. Science **2006**, *311* (5760), 506–508.
2. Mosier, N.; Wyman, C.; Dale, B.; Elander, R.; Lee, Y.Y.; Holtzapple, M.; Ladisch, M. Features of promising technologies for pretreatment of lignocellulosic biomass. Biores. Technol. **2005**, *96* (6), 673–686.
3. Teramoto, Y.; Tanaka, N.; Lee, S.H.; Endo, T. Pretreatment of eucalyptus wood chips for enzymatic saccharification using combined sulfuric acid-free ethanol cooking and ball milling. Biotechnol. Bioeng. **2008**, *99* (1), 75–85.
4. Teramoto, Y.; Lee, S.H.; Endo, T. Cost reduction and feedstock diversity for sulfuric acid-free ethanol cooking of lignocellulosic biomass as a pretreatment to enzymatic saccharification. Biores. Technol. **2009**, *100* (20), 4783–4789.

5. Ciemniecki, S.L.; Glasser, W.G. Multiphase materials with lignin. 1. Blends of hydroxypropyl lignin with poly(methyl methacrylate). Polymer **1988**, *29* (6), 1021–1029.
6. Hasegawa, D.; Teramoto, Y.; Nishio, Y. Molecular complex of lignosulfonic acid/poly(vinyl pyridine) via ionic interaction: Characterization of chemical composition and application to material surface modifications. J. Wood Sci. **2008**, *54* (2), 143–152.
7. Kadla, J.F.; Kubo, S. Miscibility and hydrogen bonding in blends of poly(ethylene oxide) and kraft lignin. Macromolecules **2003**, *36* (20), 7803–7811.
8. Kubo, S.; Kadla, J.F. Poly(ethylene oxide)/organosolv lignin blends: Relationship between thermal properties, chemical structure, and blend behavior. Macromolecules **2004**, *37* (18), 6904–6911.
9. Kubo, S.; Yoshida, T.; Kadla, J.F. Surface porosity of lignin/PP blend carbon fibers. J. Wood Chem. Technol. **2007**, *27* (3&4), 257–271.
10. Li, Y.; Mlynar, J.; Sarkanen, S. The first 85% kraft lignin-based thermoplastics. J. Polym. Sci., Part B: Polym. Phys. **1997**, *35* (12), 1899–1910.
11. Teramoto, Y.; Lee, S.H.; Endo, T. Phase structure and mechanical property of blends of organosolv lignin alkyl esters with poly(ε-caprolactone). Polym. J. **2009**, *41* (3), 219–227.
12. Kaplan, D.S. Structure-property relationships in copolymers to composites: Molecular interpretations of the glass transition phenomemon. J. Appl. Polym. Sci. **1976**, *20* (10), 2615–2629.
13. Nishio, Y.; Roy, S.K.; Manley, R.S. Blends of cellulose with polyacrylonitrile prepared from *N*,*N*-dimethylacetamide lithium-chloride solutions. Polymer **1987**, *28* (8), 1385–1390.
14. Nishio, Y.; Manley, R.S. Cellulose/poly(vinyl alcohol) blends prepared from solutions in *N*,*N*-dimethylacetamide lithium-chloride. Macromolecules **1988**, *21* (5), 1270–1277.
15. Utracki, L.A. *Polymer Alloys and Blends*; Hanser Gardner Publications: Munich, 1990.
16. Masson, J.F.; Manley, R.S. Cellulose poly(4-vinylpyridine) blends. Macromolecules **1991**, *24* (22), 5914–5921.
17. Nishio, Y. Hyperfine composites of cellulose with synthetic polymers. In *Cellulose Polymers, Blends, and Composites*; Gilbert, R.D., Ed.; Hanser: Munich, New York, 1994; 95–113.
18. Grobelny, J.; Rice, D.M.; Karasz, F.E.; MacKnight, W.J. High-resolution solid-state C-13 nuclear magnetic resonance study of polybenzimidazole/polyimide blends. Macromolecules **1990**, *23* (8), 2139–2144.
19. Zhang, X.Q.; Takegoshi, K.; Hikichi, K. High-resolution solid-state C-13 nuclear magnetic resonance study on poly(vinyl alcohol)/poly(vinylpyrrolidone) blends. Polymer **1992**, *33* (4), 712–717.
20. Miyashita, Y.; Kimura, N.; Suzuki, H.; Nishio, Y. Cellulose/poly(acryloyl morpholine) composites: Synthesis by solution coagulation bulk polymerization and analysis of phase structure. Cellulose **1998**, *5* (2), 123–134.
21. Nishio, Y.; Matsuda, K.; Miyashita, Y.; Kimura, N.; Suzuki, H. Blends of poly(ε-caprolactone) with cellulose alkyl esters: Effect of the alkyl side-chain length and degree of substitution on miscibility. Cellulose **1997**, *4* (2), 131–145.

Downloaded At: 11:56 25 January 2011

22. Kusumi, R.; Inoue, Y.; Shirakawa, M.; Miyashita, Y.; Nishio, Y. Cellulose alkyl ester/poly(ε-caprolactone) blends: Characterization of miscibility and crystallization behaviour. Cellulose **2008**, *15* (1), 1–16.
23. Khambatta, F.B.; Warner, F.; Russell, T.; Stein, R.S. Small-angle X-ray and light-scattering studies of morphology of blends of poly(ε-caprolactone) with polyvinyl chloride). J. Polym. Sci., Part B: Polym. Phys. **1976**, *14* (8), 1391–1424.
24. Cullity, B.D. In *Elements of X-Ray Diffraction*, Addison-Wesley: Massachusetts, 1978; 284.
25. Nielsen, L.E. *Mechanical Properties of Polymers and Composites*. Marcel Dekker: New York, 1974.
26. MacKnight, W.J.; Karasz, F.E.; Fried, J.R. *Solid State Transition Behaviour of Blends*. Academic Press: New York, 1978; Vol. 1, 185–242.
27. Thielemans, W.; Wool, R.P. Lignin esters for use in unsaturated thermosets: Lignin modification and solubility modeling. Biomacromolecules **2005**, *6* (4), 1895–1905.
28. McBrierty, V.J.; Douglass, D.C. Recent advances in the NMR of solid polymers. J. Polym. Sci., Part D: Macromol. Rev. **1981**, *16*, 295–366.
29. Clauss, J.; Schmidt-Rohr, K.; Spiess, H.W. Determination of domain sizes in heterogeneous polymers by solid-state NMR. Acta Polym. **1993**, *44* (1), 1–17.
30. Asano, A.; Takegoshi, K. Polymer blends and miscibility. In *Solid State NMR of Polymers*; Ando, I.; Asakura, T., Eds.; Elsevier: Amsterdam, 1998; 351–414.
31. Spiegel, S.; Schmidt-Rohr, K.; Boeffel, C.; Spiess, H.W. ^{1}H spin diffusion coefficients of highly mobile polymers. Polymer **1993**, *34* (21), 4566–4569.
32. Henrichs, P.M.; Tribone, J.; Massa, D.J.; Hewitt, J.M. Blend miscibility of bisphenol A polycarbonate and poly(ethylene terephthalate) as studied by solid-state high-resolution carbon-13 NMR spectroscopy. Macromolecules **1988**, *21* (5), 1282–1291.
33. Miyoshi, T.; Takegoshi, K.; Hikichi, K. High-resolution solid-state ^{13}C nuclear magnetic resonance study of a polymer complex: Poly(methacrylic acid)/poly(ethylene oxide) Polymer **1996**, *37* (1), 11–18.
34. Schantz, S. Structure and mobility in poly(ethylene oxide)/poly(methyl methacrylate) blends investigated by 13C solid-state NMR. Macromolecules **1997**, *30* (5), 1419–1425.

Downloaded At: 11:56 25 January 2011